IL NUOVO CIMENTO **40 C** (2017) 201
DOI 10.1393/ncc/i2017-17201-8

COLLOQUIA: Physics in Collision 2017

Precision measurements of electroweak parameters at the LHC

ALEXANDER A. SAVIN(*)
University of Wisconsin-Madison - Madison WI 53706-1390, USA

received 6 April 2018

Summary. — A set of selected precise measurements of the SM parameters from the LHC experiments is discussed. Results on W-mass measurement and forward-backward asymmetry in production of the Drell-Yan events in both dielectron and dimuon decay channels are presented together with results on the effective mixing angle measurements. Electroweak production of the vector bosons in association with two jets is discussed.

1. – Introduction

The electroweak (EW) measurements are playing an important role at the LHC. The global standard model (SM) parameters: vector boson masses, $\sin\theta_W$ are measured and provide important input to the models and global fits. The measured cross sections allow better understanding of the SM predictions and backgrounds to the searches beyond the SM. Recently available predictions at the next-to-next-to-leading order (NNLO) in QCD and next-to-leading order (NLO) in EW require for comparisons high-precision measurements with well-understood sources of the experimental and theoretical systematic uncertainties. These proceedings cover only few selected SM measurements performed by the ATLAS [1], LHCb [2, 3], and CMS [4] Collaborations.

2. – Measurement of the W mass

The available data sample of W events at the LHC at $\sqrt{s} = 7$ TeV is by an order of magnitude larger then that used for the CDF and D0 W-mass measurements [5-7], but the measurement of m_W at the LHC is affected by the fact that approximately 25% (compared to $\approx 5\%$ at Tevatron) of the inclusive W-boson production rate is induced by at least one s- or c-quark, thus making the measurement sensitive to the strange- and charm-quark parton distribution functions (PDFs) of the proton.

(*) On behalf of the ATLAS, LHCb, and CMS Collaborations.

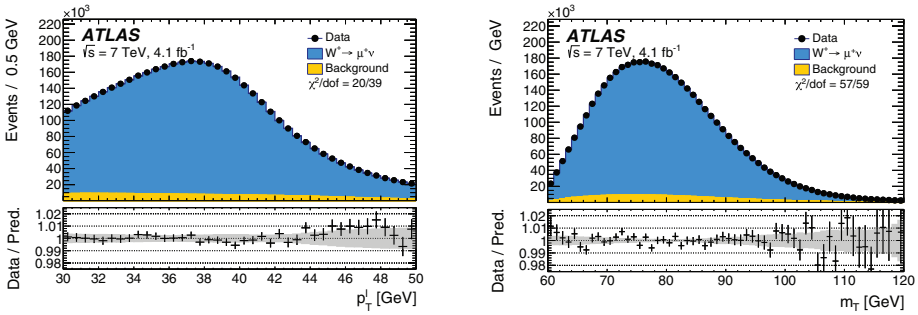

Fig. 1. – The p_T^l (left) and m_T (right) distributions for W events in the muon decay channel. The data are compared to the simulation including signal and background contributions. For simulated distributions, m_W is set according to the overall measurement result. The lower panels show the data-to-prediction ratios, the error bars show the statistical uncertainty, and the band shows the systematic uncertainty of the prediction. The χ^2 values displayed in each figure account for all sources of uncertainty and include the effects of bin-to-bin correlations induced by the systematic uncertainties [8].

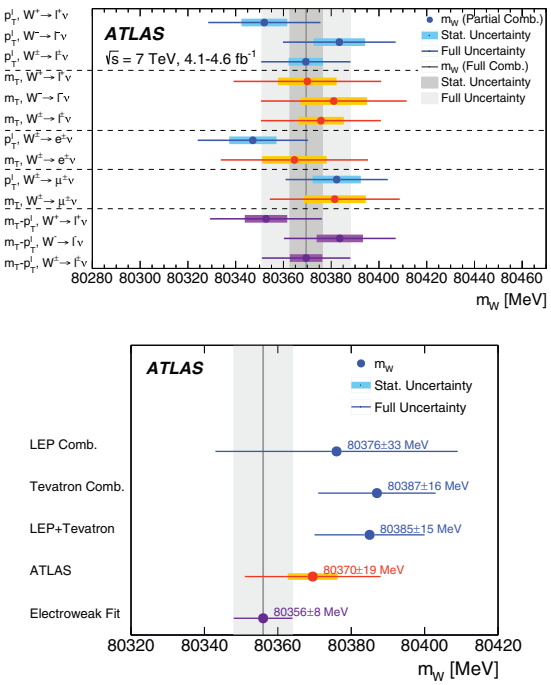

Fig. 2. – Upper plot: Overview of the m_W determinations from the p_T^l and m_T distributions, and for different combinations. The horizontal lines and bands show the statistical and total uncertainties of the individual determinations. The combined result and its statistical and total uncertainties are also indicated (vertical line and bands). Bottom plot: The measured value of m_W is compared to other published results and result of the global fit [8].

Other important aspects are the theoretical description of electroweak corrections, in particular the modelling of photon radiation from the W- and Z-boson decay leptons, and the modelling of the relative fractions of helicity cross sections in the Drell-Yan (DY) processes. The W mass for the first time at the LHC is measured by the ATLAS Collaboration [8] in $W \to \mu\nu, e\nu$ decays by fitting the measured distributions of the lepton transverse momentum, p_T^l, and W transverse mass, m_T, to the best known theoretical predictions tuned to describe the responce of the ATLAS detector. Figure 1 presents the distributions obtained in muon W decay channel. The simulation describes the data extremely well after all correction procedures described in detail in ref. [8].

The results of the fits are presented in fig. 2. The upper plot shows the measurements in different decay channels using different distributions, compared to the combined value of $m_W = 80369.5 \pm 6.8(\text{stat}) \pm 10.6(\text{syst}) \pm 13.6(\text{theo})\,\text{MeV} = 80369.5 \pm 18.5\,\text{MeV}$. The bottom plot shows comparison to the previous measurements and result of the global fit. The accuracy achieved by the first ATLAS measurement can be compared to the 15 MeV precission of the combined Tevatron measurement [7] and 8 MeV precission of the global fit result [9].

3. – Forward-backward asymmetry in Drell-Yan production and effective mixing angle measurements

The presence of both vector and axial-vector couplings of electroweak bosons to fermions lead to a forward-backward asymmetry A_{FB} in the production of DY lepton pairs. The A_{FB} is defined as $A_{FB} = \frac{\sigma_F - \sigma_B}{\sigma_F + \sigma_B}$, where $\sigma_{F(B)}$ is the total cross section for the forward ($\cos\theta^* > 0$) and backward ($\cos\theta^* < 0$) events. To reduce the uncertainties due to the transverse momentum of the incoming quarks, the measurements use the Collins-Soper (CS) frame [10]. In the recent CMS measurement [11] at $\sqrt{s} = 8\,\text{TeV}$ the DY events were detected in decays to electron and muon pairs, with lepton transverse momentum, p_T, above 20 GeV and pseudorapidity $|\eta| < 2.4$ for muons, while for electrons the region was extended up to $|\eta| < 5$ by using forward hadron (HF) calorimeter for the electrons identification. The measurement is performed as a function of dilepton mass in bins of rapidity, y, of the dilepton system. The extended region in y for electron pairs is shown in fig. 3 (left). The data are well described by the simulation convoluted with

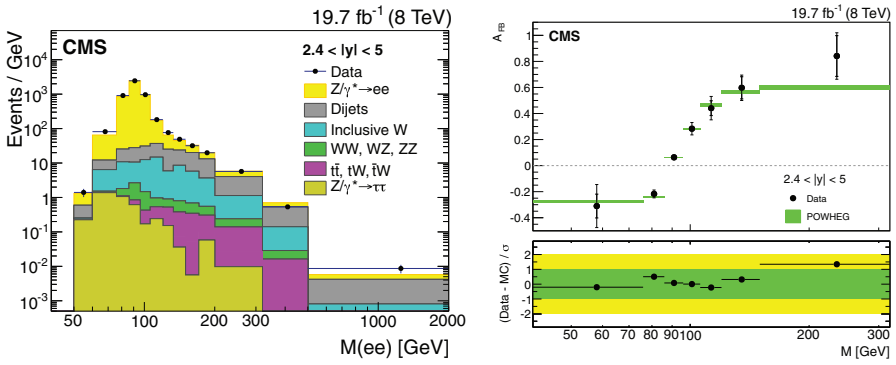

Fig. 3. – Left: The dilepton mass distributions for electron decay channels, for events with $2.4 < |y| < 5$. Right: The unfolded A_{FB} distributions in the forward region for dielectron decay channel [11].

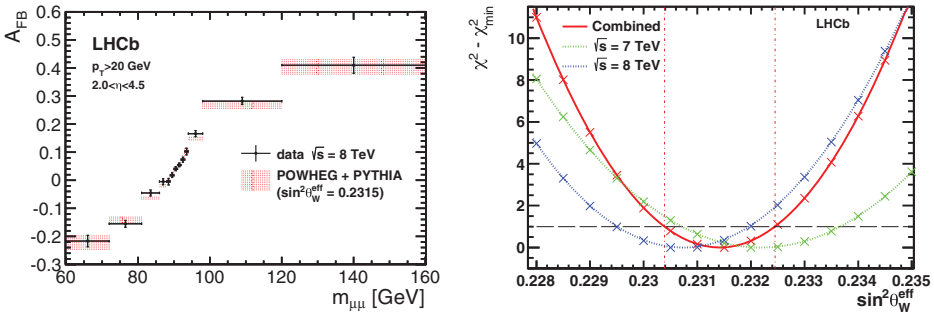

Fig. 4. – Left: The A_{FB} as a function of the dimuon invariant mass. Right: Difference between the χ^2 and the minimum χ^2 obtained by comparing the measured and predicted A_{FB} distribution for different values of $\sin^2\theta_W^{eff}$ [13].

data-driven background estimates. The backgrounds are relatively small. The major experimental uncertainties arise from the electron and muon energy corrections and from the unfolding procedure. The mass resolution in the forward region is not as good as in the central one, but this region is important since the ambiguity of the quark direction is lower at higher y and the dilution of A_{FB} is therefore smaller.

The A_{FB} measurement is performed as a function of dilepton mass in bins of rapidity. The unfolded A_{FB} distributions in the forward region for dielectron decay channel is shown in fig. 3 (right). The measured distributions agree well with the POWHEG predictions. Because A_{FB} in the forward rapidity region is less diluted, the measured A_{FB} quantity is closer to the parton-level asymmetry after the unfolding process, than it is in the central rapidity regions.

Measurement of the backward-forward asymmetry is used for extraction of the effective mixing angle. Such measurements were performed by all three experiments ATLAS [12], LHCb [13] and CMS [14, 15]. The LHCb potentially has higher power for measuring the effective mixing angle, than ATLAS and CMS, since it naturally collects events in the forward region, $2 < \eta < 5$. Figure 4, left, shows the A_{FB} as a function of dimuon mass as measured in LHCb. Both muons are required to be within $2.0 < \eta < 4.5$ and have transverse momentum greater than 20 GeV. The measurements are performed with two data samples, at $\sqrt{s} = 7$ and 8 TeV, with luminosities of 1 and 2 fb^{-1}, respectively. The A_{FB} as a function of the dimuon invariant mass is compared with several sets of SM predictions generated with POWHEG for values of $\sin^2\theta_W^{eff}$ ranging from 0.22 to 0.24. The Z-boson mass and electromagnetic coupling constant were fixed to their PDG values, NNPDF2.3 PDF set [16] was used with the strong coupling constant of 0.118. The agreement between data and predictions is quantified using χ^2 value, taking into account statistical, systematic and theoretical uncertainties, and correlations between mass bins. A quadratic function is fitted to the χ^2 as shown in fig. 4, right. The interval in $\sin^2\theta_W^{eff}$ corresponding to variation of one unit in χ^2 is quoted as the uncertainty. Combination of 7 and 8 TeV results obtained by calculating the full covariance matrix for all uncertainties yields the value $\sin^2\theta_W^{eff} = 0.23142 \pm 0.00073(\text{stat}) \pm 0.00052(\text{sys}) \pm 0.00056(\text{theo})$.

The most recent CMS effective-weak-mixing-angle measurement [15] significantly improves statistical and systematic uncertainties of the previous LHC measurements. It uses the same data set collected at $\sqrt{s} = 8$ TeV as in ref. [11], but with improved calibration of the lepton momentum/energy scale. Figure 5, left, presents the dimuon mass distribution

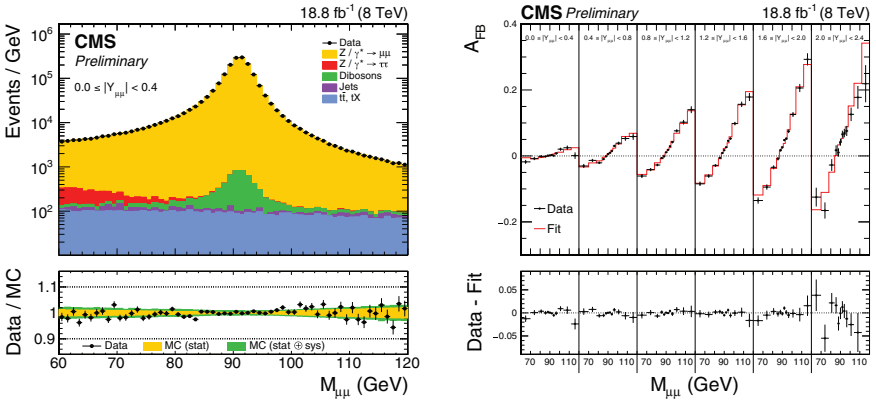

Fig. 5. – Left: The dilepton mass distributions for muon decay channels, for events with $0 < |y| < 0.4$. Right: The dimuon unfolded A_{FB} distributions in bins of rapidity [15].

in the central region. The right plot shows the weighted A_{FB} distributions in bins of rapidity that are used to measure the effective mixing angle. The improved sensitivity of the measurement is achieved by assignig maximum weights to events in the region near $\cos\theta^* = 1$ that gives the best measurement of the angular coefficient A_4. Both improvements lead to significanly reduced systematic uncertainty of the measurement. The last major improvement in the analysis is the treatment of the PDF uncertainties. The PDF uncertainty becomes the largest one, after the statistical and experimental systematic uncertainties are reduced. It is estimated by repeating analysis with 100 replicas of NNPDF 3.0 PDF. The shape of the A_{FB} distribution changes for different replicas, resulting in large PDF uncertainty in the extraction of the weak mixing angle, that is performed at Z-boson mass. The effect is reduced by assigning higher weight to replicas that describe the data in the regions of low and high dimuon masses, far from the Z-boson mass in the region that is not so sensitive to the weak-mixing-angle value. Using the weighted method reduces the PDF uncertainty of the measurement by factor of 2. The resulting measured value $\sin^2\theta^{lept}_{eff} = 0.23101 \pm 0.00036(\text{stat}) \pm 0.00018(\text{syst}) \pm 0.00016(\text{theory}) \pm 0.00030(\text{pdf})$ is compared to previous measurements by different experiments in fig. 6. The CMS measurement is the most precise LHC measurement to date and is approaching in precision the Tevatron measurements.

4. – Electroweak production of vector bosons in association with two jets

Electroweak production of vector bosons is characterized by production of one, in case of W production, or two, in case of Z, leptons in the central part of the detector with two jets in backward/forward directions separated by a large rapidity gap. The major background to EW process is W/Z+jj QCD production. In the recent ATLAS Wjj analysis [17] for $\sqrt{s} = 7$ and 8 TeV, the electrons and muons are required to have $p_T > 25$ GeV, with two jets with $p_T > 80(60)$ GeV, separated by $\Delta|y| > 2$, in the presence of missing transverse energy (greater than 20 GeV) and transverse mass, $m_T > 40$ GeV. The signal region should contain only one lepton in the central region and no jets.

Predicted and observed distributions of the dijet invariant mass for events in the signal region are shown in fig. 7, left. The measurement of the fiducial EW Wjj cross section

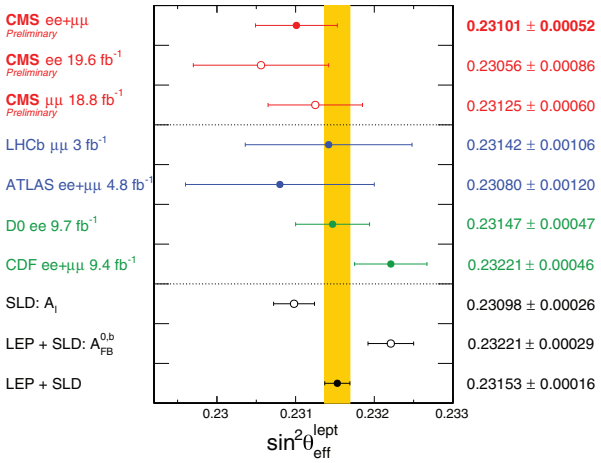

Fig. 6. – A comparison of the $\sin^2\theta_W^{eff}$ measurement at CMS and other experiments. The combined LEP and SLD measurement is indicated by the vertical yellow band [13].

in the signal region is performed with an extended joint binned likelihood fit of the dijet mass distribution for the normalization factors of the QCD and EW Powheg+Pythia8 predictions. The region at relatively low invariant mass 500–1000 GeV has low signal purity and primarily determines QCD contribution, while events with higher invariant mass have higher signal purity and mainly determine EW contribution. The interference between the processes is not included in the fit, and is instead taken as an uncertainty based on SM predictions. The measured fiducial EW cross sections $144 \pm 23(\text{stat}) \pm 23(\text{exp}) \pm 13(\text{theo})$ fb for 7 TeV and $159 \pm 10(\text{stat}) \pm 17(\text{exp}) \pm 20(\text{theo})$ fb for 8 TeV can

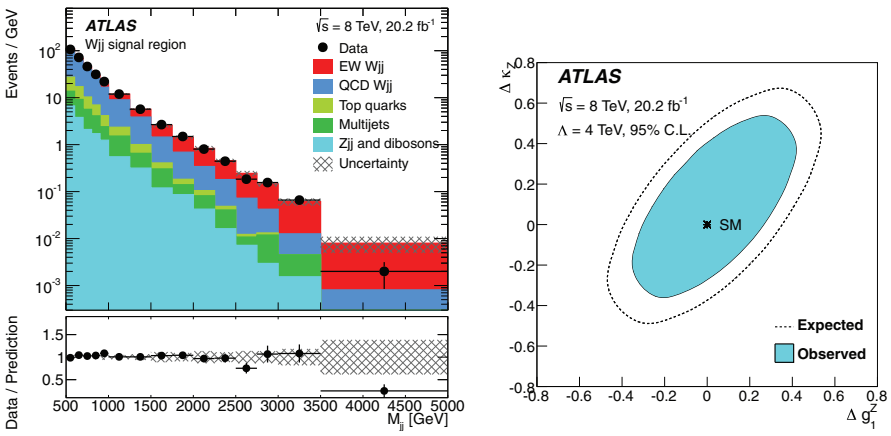

Fig. 7. – Left: Distribution of the dijet invariant mass for events in the signal region in 8 TeV data, after fitting for the yields of the individual Wjj processes. The bottom panel shows the ratio of data to predicted signal-plus-background yields. The shaded band centred at unity represents the statistical and experimental uncertainties summed in quadrature. Right: The observed (solid blue) and expected (open dashed) 95% CL allowed regions in two-parameter aTGC plane $\Delta\kappa_Z$ and Δg_1^Z [17].

be compared to predicted values of 144 ± 11 and 198 ± 12 fb for 7 and 8 TeV, respectively. The paper also includes number of differential cross section measurements and set limits on anomalous triple-gauge-boson couplings. Figure 7, right, demonstrates the observed (solid blue) and expected (open dashed) 95% confedence level (CL) allowed regions in two-parameter plane for aTGC parameters $\Delta\kappa_Z$ and Δg_1^Z.

The first measurements of the EW production of Z bosons at 13 TeV were performed by both ATLAS [18] and CMS [19] experiments. The measurements require pairs of electrons or muons, with mass within 10 (ATLAS) and 15 (CMS) GeV from the nominal Z-boson mass for leptons with $p_T > 25$(ATLAS), and 30 and 20 (CMS) GeV, and two jets with $p_T > 55$ and 45 (ATLAS) , and 50 and 30 (CMS) GeV. The dijet invariant mass for the combination of the dielectron and dimuon decay channels in the ATLAS measurement is shown in fig. 8, left. One can see that the EW relative contribution increases with dijet mass as expected but the QCD contribution still plays an important role even for very high masses. The EW cross sections measured using fit to the dijet mass distribution $119 \pm 16(\text{stat}) \pm 20(\text{syst}) \pm 2(\text{lum})(34.2 \pm 5.8 \pm 5.5 \pm 0.7)$ fb for dijet mass region above 250 (1000) GeV agree well with predicted values from Powheg+Pythia $125.2 \pm 3.4(38.5 \pm 1.5)$ fb.

To improve the precission of such measurement in CMS experiment, a boosted decision tree (BDT) is used based on set of variables like the dijet pseudorapidity opening $\Delta\eta_{jj}$, the dijet transverse momentum and others. The BDT is trained to achieve the best separation between EW and DY production and the resulting distributions for dimuon channel are shown in fig. 8, right. As expected, the BDT provides better separation between the signal and the background than the dijet mass distribution alone. The measured EW cross section by combining electron and muon channels: $552 \pm 19(\text{stat}) \pm 55(\text{syst})$ fb agrees well with the SM prediction, 543 ± 24 fb and has much improved statistical and systematic uncertainties compared to the previously discussed measurement.

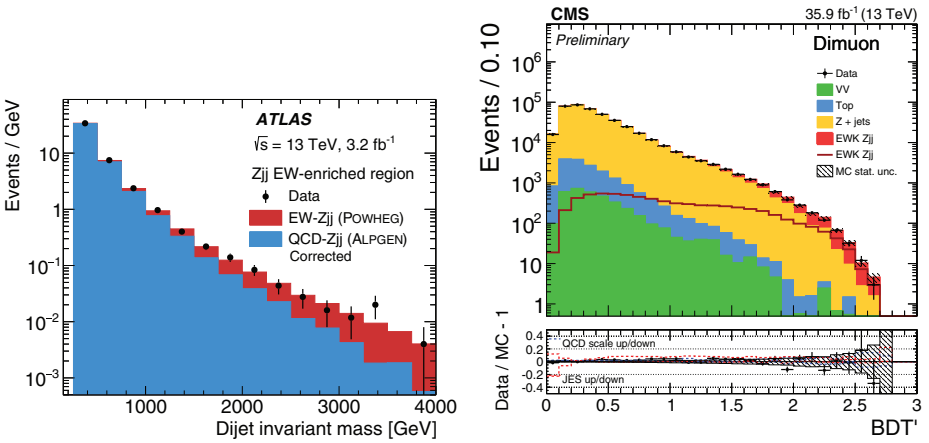

Fig. 8. – Left: Invariant mass of the dijet system for data and simulated events measured by the ATLAS experiment [18]. The contributions from reducible backgrounds is subtracted. The EW signal and QCD background are shown stacked, with data points superimposed. Right: Distribution for the BDT discriminant in dimuon events as measured by the CMS experiment [19].The lower panel shows the relative difference between the data and expectations as well as the uncertainty envelopes for JES and QCD scales uncertainties.

5. – Summary

These proceedings present only some selected EW measurements, there were more contributions presented at this conference that covered other EW topics. In most of the cases the statistical uncertainties do not dominate the precision of the measurements and better understanding of systematics, and in some cases theoretical uncertainties, are required.

* * *

The University of Wisconsin-Madison would like to acknowledge the U.S. Department of Energy (DOE) and the National Science Foundation (NSF) for funding their contribution to this research.

REFERENCES

[1] ATLAS Collaboration , *JINST*, **3** (2008) S08003.
[2] LHCb Collaboration, *JINST*, **3** (2008) S08005.
[3] LHCb Collaboration, *Int. J. Mod. Phys. A*, **3** (2015) 1530022.
[4] CMS Collaboration, *JINST*, **3** (2008) S08004.
[5] CDF Collaboration, *Phys. Rev. D*, **64** (2001) 052001.
[6] D0 Collaboration, *Phys. Rev. D*, **66** (2002) 012001.
[7] CDF and D0 Collaborations, *Phys. Rev. D*, **70** (2004) 092008.
[8] ATLAS Collaboration, arXiv:1701.07240 (2017).
[9] de Blas J. *et al.*, *JHEP*, **12** (2016) 135.
[10] Collins J. C. and Soper D. E., *Phys. Rev. D*, **16** (1977) 2219.
[11] CMS Collaboration, *Eur. Phys. J. C*, **76** (2016) 325.
[12] ATLAS Collaboration, *JHEP*, **09** (2015) 049.
[13] LHCb Collaboration, *JHEP*, **11** (2015) 190.
[14] CMS Collaboration, *Phys. Rev. D*, **84** (2011) 112002.
[15] CMS Collaboration, `CMS-SMP-PAS-16-007,https://cds.cern.ch/record/2273392` (2017).
[16] Ball R. D. *et al.*, *Nucl. Phys. B*, **867** (2013) 244.
[17] ATLAS Collaboration, *Eur. Phys. J. C*, **77** (2017) 474.
[18] ATLAS Collaboration, `CERN-EP-2017-115,https://cds.cern.ch/record/2286337` (2017).
[19] CMS Collaboration, `CMS-PAS-SMP-16-018,https://cds.cern.ch/record/2261499` (2017).